Analysis of electron transport in a fullerene derivative: evidence for the absence of correlated disorder

L. ZHANG, J. Y. LIU*, L. G. WANG*, Y. J. WANG, Y. GUO, G. C. WANG
School of Electrical Engineering and Automation, Henan Polytechnic University, Jiaozuo, 454000, People's Republic of China

In this paper, the electron transport in a fullerene derivative indene-C60 bisadduct (ICBA), which is frequently used in organic solar cells and transistors, is studied. From an analysis of the layer thickness and temperature dependence of the current density-voltage ($J-V$) characteristics of ICBA electron-only devices, it is found that consistent descriptions with equal quality are obtained using both the improved extended Gaussian disorder model (IEGDM) and the extended correlated disorder model (ECDM), within which spatial correlations between the transport site energies are absent and are included, respectively. Based on a comparison of the model parameters as obtained from both models, we view the more realistic intersite distance obtained using the IEGDM (2.7 nm) compared to the value obtained using the ECDM (0.3 nm) as an indication that in ICBA correlations between the transport site energies are absent. Distinguishing correlated from uncorrelated disorder, which we achieve on the basis of the intersite distance, is shown to be highly relevant for the development of quantitative organic electron device models.

(Received February 23, 2020; accepted June 16, 2020)

Keywords: Electron transport, Fullerene derivative, Intersite distance, Spatially correlated disorder

1. Introduction

Organic semiconductors are a promising alternative to conventional inorganic semiconductors, because of their ease of processing, flexibility, and low cost. However, charge transport in organic semiconductors is governed by hopping conduction, leading to charge carrier mobilities and conductivities that are orders of magnitude lower as compared to inorganic semiconductors. Fullerenes and their derivatives are widely used in organic solar cells, in organic field-effect transistors, and as electron-transport layers in hybrid perovskite photovoltaic cells, owing to their excellent electron-transport capabilities [1–3]. By functionalizing fullerenes with side groups, their solubility and energy levels can be tuned, enabling their use in solution-processed electronic devices [4–6]. With regard to electron transport, fullerenes exhibit mobilities that are among the highest in organic semiconductors [7] and exceptionally long electron diffusion lengths have been observed [8]. A further detailed understanding of the charge transport in these fullerenes and their derivatives is a prerequisite for the improvement of organic device performance. The most important parameter for describing the charge transport is the charge carrier mobility μ, which quantifies how easily charge carriers move when an electric field is applied.

It is widely agreed that the charge carrier mobility in organic semiconductors is determined by hopping between localized states. However, the development of charge transport models with predictive value is hampered by a lack of consensus about the type of energetic disorder: completely random or with correlation between the transport site energies. In the early modeling introduced by Bässler et al. [9, 10], the random energies were described by a Gaussian density of states (DOS), leading to the Gaussian disorder model (GDM), within which spatial correlations between the transport site energies are absent. Alternatively, it was suggested that the presence of dipole moments can give rise to spatial correlation between the site energies [11, 12], leading to the correlated disorder model (CDM). Later, it was realized that, apart from the dependence of the mobility μ on the electric field E and temperature T, there is a strong dependence on the carrier concentration p [13–15], giving rise to the extended versions of the GDM and CDM, the EGDM [16] and ECDM [17], respectively. Furthermore, it should be noted that the EGDM, having a non-Arrhenius temperature dependence $\ln(\mu) \propto 1/T^2$, can only well describe the charge transport at low carrier densities. To better describe the charge transport, we proposed an improved model within which the temperature dependence of the mobility based on both the non-Arrhenius temperature dependence and Arrhenius temperature dependence $\ln(\mu) \propto 1/T$, leading to the improved extended Gaussian disorder model (IEGDM) [18]. It has been shown that the improved mobility model can rather well describe the charge

transport in various organic semiconductors [19-21].

For the GDM and CDM, key issues are the roles of the energetic disorder of the states where the charge carrier hopping occur, assuming a Gaussian density of state (DOS) with random and spatially correlated energetic disorder, respectively. Being able to make a distinction between various models, to determine the type of disorder and to accurately extract the materials parameters that determine the mobility in organic semiconductors are of great importance to the development of quantitative device models and the rational design of organic devices. However, analyses of measured current density versus voltage ($J-V$) curves of sandwich-type devices based on several polymers have been successfully carried out using the EGDM [22–25], whereas for several small-molecule materials, a more consistent analysis was obtained by using the ECDM [26, 27]. The question now arises whether a successful analysis of current density versus voltage ($J-V$) characteristics of a certain material using the EGDM or ECDM would already convincingly proof that the disorder is completely random or correlated, respectively. To date, it has remained unclear to what extent it is possible to make a distinction between the EGDM and ECDM, and the type of disorder (random or spatially correlated).

In this paper, the $J-V$ characteristics of the electron transport and the possible presence of spatially correlated disorder in a fullerene derivative indene-C60 bisadduct (ICBA) are investigated. We address the above question by analyzing the layer thickness and temperature dependence of the $J-V$ characteristics for ICBA electron-only devices by using the IEGDM and ECDM, respectively. It is found that an equally good fit to the $J(V)$ curves can be obtained using both the IEGDM and ECDM, but a more realistic value of the intersite distance is obtained within the IEGDM (2.7nm) than within the ECDM (0.3nm). This is an indication that in fullerene derivative bisadduct ICBA spatially correlations between the transport site energies are absent.

2. Models and methods

The extended Gaussian disorder model (EGDM) has been developed by Pasveer et al. on basis of numerical transport simulations accounting for hopping on a simple cubic lattice with uncorrelated Gaussian disorder [16]. Based on the EGDM, we proposed an improved mobility model (IEGDM) in which the dependence of the mobility μ on the electric field E, carrier concentration p, and temperature T [18]. In particular, the dependence of the zero-field mobility on the carrier concentration p and temperature T is given by

$$\mu(T,p)=\mu_0(T)\exp\left[\frac{1}{2}\left(\hat{\sigma}^2-\hat{\sigma}\right)\left(2pa^3\right)^{\delta}\right], \quad (1a)$$

$$\mu_0(T)=\mu_0 c_1\exp\left(c_2\hat{\sigma}-c_3\hat{\sigma}^2\right), \quad (1b)$$

$$\delta\equiv 2\frac{\ln(\hat{\sigma}^2-\hat{\sigma})-\ln(\ln 4)}{\hat{\sigma}^2},\ \mu_0\equiv\frac{a^2\nu_0 e}{\sigma}, \quad (1c)$$

with $c_1=0.48\times10^{-9}$, $c_2=0.80$, and $c_3=0.52$. Where $\mu_0(T)$ is the mobility in the limit of zero carrier density and zero electric field, $\hat{\sigma}\equiv\sigma/k_BT$ is the dimensionless disorder parameter, σ is the width of the Gaussian density of states (DOS), a is the lattice constant (intersite distance), e is the charge of the carriers, and ν_0 is the attempt-to-hop frequency. The field dependence of the mobility is included via

$$\mu(T,p,E)=\mu(T,p)^{g(T,E)}\exp\left[c_4\left(g(T,E)-1\right)\right], \quad (2)$$

$$g(T,E)=\left[1+c_5(Eea/\sigma)^2\right]^{-1/2}, \quad (3)$$

where $g(T,E)$ is a weak density dependent function, c_4 and c_5 are weak density dependent parameters, given by

$$c_4=d_1+d_2\ln(pa^3) \quad (4a)$$

$$c_5=1.16+0.09\ln(pa^3) \quad (4b)$$

$$d_1=28.7-36.3\hat{\sigma}^{-1}+42.5\hat{\sigma}^{-2} \quad (5a)$$

$$d_2=-0.38+0.19\hat{\sigma}+0.03\hat{\sigma}^2 \quad (5b)$$

In addition to uncorrelated energetic disorder, the presence of molecular dipoles may give rise to spatial correlations in the energy landscape. Bouhassoune et al. employed the same methodology as in the EGDM, but for an energy landscape with Gaussian disorder σ that results from randomly oriented dipole moments of equal magnitude on all lattice sites, leading to the extended correlated disorder model (ECDM) [17], which can be described by the following phenomenological expression:

$$\mu(T,p,E)=\left[(\mu_{low}(T,p,E))^{q(\hat{\sigma})}+(\mu_{high}(p,E))^{q(\hat{\sigma})}\right]^{1/q(\hat{\sigma})}, \quad (6)$$

$$q(\hat{\sigma})=2.4/(1-\hat{\sigma}), \quad (7)$$

with $\mu_{low}(T,p,E)$ the mobility in the low-field limit (the average reduced field $E_{red}=eaE/\sigma\le 1$), and with $\mu_{high}(p,E)$ the mobility in the high-field limit (the average reduced field $E_{red}=eaE/\sigma\ge 1$).

$$\mu_{low}(T,p,E)=\mu_0(T)g(T,p)f(T,E,p), \quad (8)$$

where $g(T,p)$ and $f(T,E,p)$ are the dimensionless mobility enhancement functions. These functions can be written as follows:

$$\mu_0(T) = 1.0\times10^{-9}\,\mu_0 \exp(-0.29\hat{\sigma}^2), \quad (9)$$

$$g(T,p) = \begin{cases} \exp[(0.25\hat{\sigma}^2 + 0.7\hat{\sigma})(2pa^3)^{\delta}], pa^3 < 0.025 \\ g(T, 0.025a^{-3}), pa^3 \geq 0.025 \end{cases}, \quad (10)$$

$$\delta \equiv 2.3\frac{\ln(0.5\hat{\sigma}^2 + 1.4\hat{\sigma}) - 0.327}{\hat{\sigma}^2}, \quad (11)$$

$$f(T, E_{red}, p) = \exp[h(E_{red})(1.05 - 1.2(pa^3)^{r(\hat{\sigma})}) (\hat{\sigma}^{3/2} - 2)(\sqrt{1 + 2E_{red}} - 1)], \quad (12)$$

$$h(E_{red}) = 1, \quad r(\hat{\sigma}) = 0.7\hat{\sigma}^{-0.7}, \quad (13)$$

within the very low-field, $0 \leq E_{red} < 0.16 \equiv E^*_{red}$, $h(E_{red})$ can be written as

$$h(E_{red}) = \begin{cases} \frac{4}{3}\frac{E_{red}}{E^*_{red}}, (E_{red} \leq E^*_{red}/2) \\ \left[1 - \frac{4}{3}\left(\frac{E_{red}}{E^*_{red}} - 1\right)^2\right], (E^*_{red}/2 \leq E_{red} \leq E^*_{red}) \end{cases}, \quad (14)$$

$$\mu_{high}(p,E) = \frac{2.06\times10^{-9}}{E_{red}}\mu_0(1 - pa^3). \quad (15)$$

By using the above mobility models, the $J-V$ characteristics of organic electron devices can be exactly calculated by numerically solving the following equations adopting a particular uneven discretization method introduced in our previous paper [28, 29].

$$J = p(x)e\mu(T, p(x), E(x))E(x), \quad (16a)$$

$$\frac{dE}{dx} = \frac{e}{\varepsilon_0\varepsilon_r}p(x), \quad (16b)$$

$$V = \int_0^L E(x)dx, \quad (16c)$$

where x is the distance from the injecting electrode, L is the organic semiconductor layer thickness sandwiched between two electrodes, $\varepsilon_0\varepsilon_r$ is the permeability of the organic semiconductors.

3. Results and discussion

To explore the spatial correlations between the site energies and electron transport in detail, we investigate the layer thickness dependent and temperature dependent $J-V$ characteristics of electron-only devices based on the fullerene derivative indene-C60 bisadduct (ICBA) by using the IEGDM and ECDM, respectively. As previously described, the mobility in disordered semiconductors exhibiting hopping transport depends on the temperature, electric field, and charge concentration. For a system with Gaussian disorder, the mobility characteristics can be described by both the IEGDM and ECDM, which uses three input parameters: the width of the Gaussian density of states distribution σ, the intersite distance a, and a mobility prefactor μ_0. The σ mainly controls its temperature and charge concentration dependence, a predominantly affects its field dependence, and the mobility prefactor determines the magnitude of the mobility.

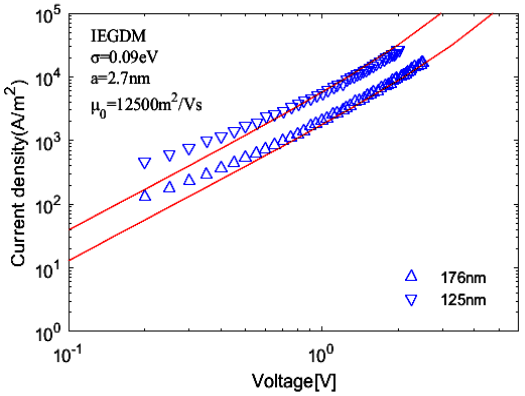

Fig. 1. Thickness dependent J-V characteristics of ICBA electron-only devices at room temperature. Symbols are experimental measurements from Ref. [25]. Lines are the numerically calculated results based on the IEGDM (color online)

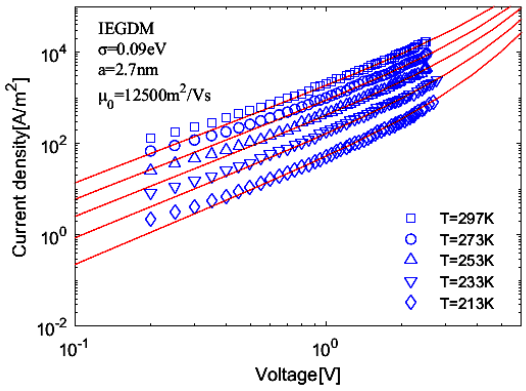

Fig. 2. Temperature dependent J-V characteristics of an electron-only device based on ICBA with a layer thickness of 176 nm. Symbols are experimental data from Ref. [25]. Lines are the numerically calculated results based on the IEGDM (color online)

Fig. 1 shows the thickness dependent $J-V$ characteristics of electron-only devices with ICBA layer thickness of 125 nm and 176 nm at room temperature. Apparently, the experimental data from Ref. [25] can be well described by using the IEGDM, within which an optimal fit can be obtained using a single parameter set of a =2.7 nm, σ =0.09 eV, and μ_0 =12500 m^2/Vs. Fig. 2 depicts the temperature dependent $J-V$ characteristics of an electron-only device based on ICBA

with a layer thickness of 176 nm. It is obviously that the temperature dependent electron current could also be accurately described within the IEGDM using the same parameters as the thickness dependent $J(V)$ curves. For the model parameters, the value of the disorder parameter σ is equal to the value used by Kotadiya et al. [25]. The value of intersite distance a found in this work is very close to the typical value of fullerenes and their derivatives [25, 30]. Apparently, our numerical simulations based on the IEGDM are in good agreement with the experimental measurements, which suggests that the IEGDM is suitable to study the electron transport in the bisadduct fullerene ICBA.

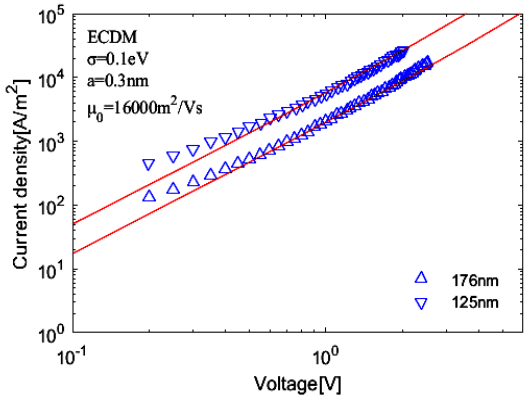

Fig. 3. Thickness dependent J-V characteristics of ICBA electron-only devices at room temperature. Symbols are experimental measurements from Ref. [25]. Lines are the numerically calculated results based on the ECDM (color online)

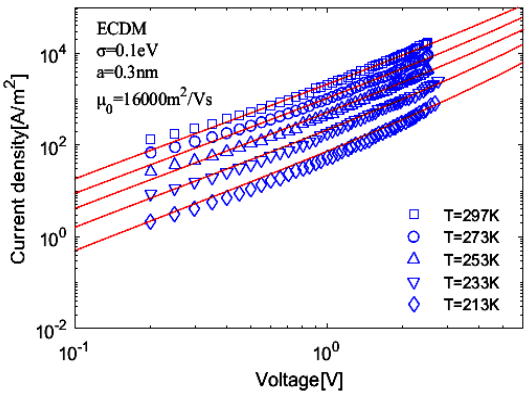

Fig. 4. Temperature dependent J-V characteristics of an electron-only device based on ICBA with a layer thickness of 176 nm. Symbols are experimental data from Ref. [25]. Lines are the numerically calculated results based on the ECDM (color online)

As a next step, we consider the question whether the ECDM can also describe the $J-V$ characteristics of ICBA electron-only devices with various layer thicknesses and temperatures as successfully as the IEGDM. When employing the ECDM, we address the question whether site-energy correlations with this specific correlation function are present in ICBA. Here, we re-analyse these experimental data from Ref. [25] for ICBA electron-only devices by using the ECDM. Fig. 3 and Fig.4 show the layer thickness dependent and temperature dependent $J-V$ characteristics of ICBA electron-only devices, respectively. Obviously, the layer thickness dependent and temperature dependent $J-V$ characteristics of ICBA electron-only devices can also be well described within the ECDM only using a single set of parameters, a =0.3 nm, σ =0.1 eV, and μ_0 =16000 m^2/Vs. It is concluded that the ECDM can also provide a good description for the electron transport in ICBA, provided that a much smaller intersite distance is assumed within the ECDM (0.3 nm) than within the EGDM (2.7 nm).

It can be seen from Figs. 1-4 that equally good descriptions of the layer thickness dependent and temperature dependent $J-V$ characteristics of ICBA electron-only devices can be obtained within both the IEGDM and ECDM. For both models, the shape of the $J(V)$ curves depends on only two temperature and thickness independent parameters, σ and a. Varying the mobility in the zero-density and zero-field limit $\mu_0(T)$, gives rise to an overall vertical shift of the $J(V)$ curves, but does not affect the shape. The optimal fitting parameter set for each model is obtained as follows. We determine the fitting errors between the experimental and calculated $J(V)$ curves for each layer thickness and temperature. The total error is calculated as a sum of mean square errors of the fits for all layer thicknesses and temperatures. By minimizing this total error, we obtain the optimal model parameter set. For the IEGDM, the value of a and σ obtained in this work are 2.7 nm and 0.09 eV, and for the ECDM, a =0.3 nm and σ =0.1 eV are obtained. By optimizing the position of the $J(V)$ curves along the vertical axes, the optimal temperature dependent μ_0 can be determined for the IEGDM (12500 m^2/Vs) and ECDM (16000 m^2/Vs), respectively.

The key parameters in both the IEGDM and ECDM are the strength of the energetic disorder, quantified by the width of the DOS σ, and the average hopping site distance a. The optimal fit values of a as obtained from the IEGDM and ECDM are very different, viz. 2.7 nm and 0.3 nm, respectively. The value of a found for the IEGDM is very close to the typical value of fullerenes and their derivatives, slightly larger than the result reported by Eersel et al. for PCBM (2.54 nm) [30], and slightly smaller than the value obtained by Kotadiya et al. for ICBA (3.0 nm) [25]. However, the value of a found for the ECDM may be considered as unrealistically small (10 times lower than the typical value). This suggests that for ICBA the energies of the sites in between which hopping takes place are uncorrelated. The values obtained for σ does not change this point of view. For disordered organic semiconductors, the Gaussian density of states σ is typically observed to fall in the range 0.06-0.16 eV, the optimal values of σ obtained within both models (0.09 eV for the IEGDM

and 0.1 eV for the ECDM) are physically realistic.

4. Summary and conclusions

In summary, the electron transport and the possible presence of spatially correlated disorder in a fullerene derivative bisadduct ICBA are investigated. It is found that the thickness dependent and temperature dependent $J-V$ characteristics of the ICBA electron-only devices can be accurately described using both the IEGDM and ECDM, within which spatial correlations between the transport site energies are absent and are included, respectively. Apparently, a successful analysis of the $J(V)$ curves using above two models does not yet convincingly prove that the disorder is completely random or correlated. Especially, for the material studied, we argue that the most significant difference between the two sets of optimal fit parameters is an observed large difference between the intersite distance a. The parameter a =2.7 nm is found for the IEGDM, whereas the value of a obtained for the ECDM is 0.3 nm. The intersite distance found using the IEGDM is very close to the typical value of fullerenes and their derivatives, whereas the value of a found for the ECDM may be considered as unrealistically small. This indicates that for the ICBA studied correlations between the site energies are absent or insignificant. Finally, we mention that the present work is useful to build up the quantitative organic electron device models.

Acknowledgements

This work is supported by the Young Key Teacher Program of Henan Polytechnic University Grant No. 2019XQG-17, the Doctoral Scientific Research Foundation of Henan Polytechnic University Grant No. B2014-022 and No.B2017-20, and the Key Scientific Research Project of Colleges and Universities of Henan Grant No. 18A470014.

References

[1] J. E. Anthony, A. Facchetti, M. Heeney, S. R. Marder, X. Zhan, Adv. Mater. **22**, 3876 (2010).
[2] J. Liu, L. Qiu, G. Portale, M. Koopmans, G. ten Brink, J. C. Hummelen, L. J. A, Koster, Adv. Mater. **29**, 1701641 (2017).
[3] G. Yang, H. Tao, P. Qin, W. Ke, G. Fang, J. Mater. Chem. A **4**, 3970 (2016).
[4] G. Yu, J. Gao, J. C. Hummelen, F. Wudl, A. J. Heeger, Science **270**, 1789 (1995).
[5] M. Lenes, G. A. H. Wetzelaer, F. B. Kooistra, S. C. Veenstra, J. C. Hummelen, P. W. M. Blom, Adv. Mater. **20**, 2116 (2008).
[6] Y. He, H. Y. Chen, J. Hou, Y. Li, J. Am. Chem. Soc. **132**, 1377 (2010).
[7] H. Li, B. C. K. Tee, J. J. Cha, Y. Cui, J. W. Chung, S. Y. Lee, Z. Bao, J. Am. Chem. Soc. **134**, 2760 (2012).
[8] Q. Burlingame, C. Coburn, X. Che, A. Panda, Y. Qu, S. R. Forrest, Nature **554**, 77 (2018).
[9] L. Pautmeier, R. Richert, H. Bässler, Synth. Met. **37**, 271 (1990).
[10] H. Bässler, Phys. Status Solidi (b) **175**, 15 (1993).
[11] Y. Gartstein, E. Conwell, Chem. Phys. Lett. **245**, 351 (1995).
[12] S. V. Novikov, D. H. Dunlap, V. M. Kenkre, P. E. Parris, A. V. Vannikov, Phys. Rev. Lett. **81**, 4472 (1998).
[13] Y. Roichman, N. Tessler, Synth. Met. **135**, 443 (2003).
[14] C. Tanase, E. J. Meijer, P. W. M. Blom, D. M. de Leeuw, Phys. Rev. Lett. **91**, 216601 (2003).
[15] R. Coehoorn, W. F. Pasveer, P. A. Bobbert, M. A. J. Michels, Phys. Rev. B **72**, 155206 (2005).
[16] W. F. Pasveer, J. Cottaar, C. Tanase, R. Coehoorn, P. A. Bobbert, P. W. M. Blom, D. M. de Leeuw, M. A. J. Michels, Phys. Rev. Lett. **94**, 206601 (2005).
[17] M. Bouhassoune, S. L. M. van Mensfoort, P. A. Bobbert, R. Coehoorn, Org. Electron. **10**, 437 (2009).
[18] L. G. Wang, H. W. Zhang, X. L. Tang, C. H. Mu, Eur. Phys. J. B **74**, 1 (2010).
[19] I. Katsouras, A. Najafi, K. Asadi, A. J. Kronemeijer, A. J. Oostra, L. J. A. Koster, D. M. de Leeuw, P. W. M. Blom, Org. Electron. **14**, 1591 (2013).
[20] L. G. Wang, M. L. Liu, J. J. Zhu, L. F. Cheng, Optoelectron. Adv. Mat. **11**, 202 (2017).
[21] B. B. Cui, L. G. Wang, M. L. Liu, Y. Guo, W. Zhang, Optoelectron. Adv. Mat. **12**, 512 (2018).
[22] S. L. M. van Mensfoort, S. I. E. Vulto, R. A. J. Janssen, R. Coehoorn, Phys. Rev. B **78**, 085208 (2008).
[23] J. C. Blakesley, H. S. Clubb, N. C. Greenham, Phys. Rev. B **81**, 045210 (2010).
[24] P. Kordt, J. J. M. van der Holst, M. A. Helwi, W. Kowalsky, F. May, A. Badinski, C. Lennartz, D. Andrienko, Adv. Funct. Mater. **25**, 1955 (2015).
[25] N. B. Kotadiya, P. W. M. Blom, G. A. H. Wetzelaer, Phys. Rev. Applied **11**, 024069 (2019).
[26] S. L. M. van Mensfoort, V. Shabro, R. J. de Vries, R. A. J. Janssen, R. Coehoorn, J. Appl. Phys. **107**, 113710 (2010).
[27] S. L. M. van Mensfoort, R. J. de Vries, V. Shabro, H. P. Loebl, R. A. J. Janssen, R. Coehoorn, Org. Electron. **11**, 1408 (2010).
[28] L. G. Wang, H. W. Zhang, X. L. Tang, Y. Q. Song, Optoelectron. Adv. Mat. **5**, 263 (2011).
[29] M. L. Liu, L. G. Wang, J. Optoelectron. Adv. M. **19**, 406 (2017).
[30] H. van Eersel, R. A. J. Janssen, M. Kemerink, Adv. Funct. Mater. **22**, 2700 (2012).

*Corresponding authors: liujy@hpu.edu.cn, wangliguo@hpu.edu.cn